Chapter 5

Displacement, flow stress, and strain rates along the central segment of the Proto-Kern Canyon Fault

Introduction

In Chapter 4, a detailed microstructural study of the Durrwood Creek segment of the Kern Canyon pendant was presented along with analyses of displacement along the ductile Proto-Kern Canyon Fault (PKCF) from both granitic S-C mylonites and metamorphic pendant rocks deformed along the shear zone. In this chapter, two displacement analyses are presented for study areas in the middle segment of the PKCF. In addition, a map analysis of stretched rocks is used to estimate the maximum dextral strike-slip displacement that could have occurred along this middle segment. Estimates of paleostresses along the PKCF are also made. Experimental studies show that the size of grains produced by dynamic recrystallization in rocks of uniform composition can be used to estimate flow stress during rock deformation (Mercier et al., 1977; Twiss, 1977; Christie et al., 1980; Koch, 1983; Ord and Christie, 1984; Hacker et al., 1990; Hacker et al., 1992; Dunlap, 1992). This section presents the results of a paleostress analysis using recrystallized grain size measurements from two quartzite samples from the middle section of the PKCF (see Plate 1 for locations).

Geologic setting

Both detailed and reconnaissance mapping were undertaken for the northern half of the PKCF, from latitudes 35˚40′ N to 36˚10′ N (Plate 1). A detailed analysis of the

northernmost segment, the Durrwood Creek map area, is presented in Chapter 4. Here we concentrate on similar rocks within the middle segment of the PKCF, from Lake Isabella to the southernmost part of the Durrwood Creek map area. The metamorphic pendants in this study area are the southern half of the Kern Canyon pendant and the northern half of the Isabella pendant (Fig. 1, Chapter 4). The details of the protoliths to these metamorphic pendant rocks are presented in Chapter 4. Igneous rocks in this study area consist of pluton suites that are, for the most part, separated by the PKCF. To the west of the PKCF are the ca. 105–102 Ma Intrusive Suite of the Kern River, the ca. 102–98 Ma Intrusive Suite of Bear Valley, and the ca. 100–96 Ma Intrusive Suite of the Needles. East of the PKCF lie the ca. 100–94 Ma Intrusive Suite of the South Fork and the ca. 95–84 Ma Intrusive Suite of the Domelands. Details of these igneous rocks and their ages are presented in Chapter 2. Crucial to study of displacement along this middle segment of the PKCF are the final phases of igneous intrusions of the Domelands suite. These are the Granite of Cannell Creek and the Goldledge granite (Plate 1). Both of these are north–south elongated and ductiley deformed along the PKCF just north of Lake Isabella.

Displacement along the middle segment of the PKCF

Two shear strain–displacement analyses were performed for this section of the PKCF. The first is across S-C mylonites of the Goldledge granite just east of sample 91SS27, and the second is across S-C mylonites of the Granite of Cannell Creek just east of sample location 89SS14 (see Plate 1 for locations). These analyses were performed following the Ramsay and Graham (1970) equation presented in Chapter 4 (Fig. 1). Because the curves were manually fitted to the data, the total displacement was calculated

not by integrating for the area under the curve but by summing the individual shear displacements with the formula

$$d = {}_0\Sigma^x \gamma \, \delta x \tag{4}$$

where x is the distance from the shear zone margin and d is total displacement. For the Goldledge transect, the measurements yield a total displacement of 4 km (Fig. 1a). For the Cannell Creek section, the measurements yield total displacement of 6.75 km (Fig. 1b).

The displacements across the PKCF calculated for the Cannell Creek and Goldledge granites are similar to the ~5 km displacement calculated in the Castle Rock granite of the Durrwood Creek study area (Chapter 4). However, field studies suggest that displacement could have been much greater. For one, the Cannell Creek and Goldledge granites were both being emplaced as they were sheared, and thus have elongate, tabular shapes with an aspect ratio of ~1:12. Their lengths, stretched over 14.5 km and 10.5 km, respectively, suggest that these igneous bodies could have accommodated up to 10 km of dextral shearing during emplacement.

Pendant rocks along the middle and northern sections of the PKCF also suggest a greater displacement than that indicated by the shear strain studies. Outside of the shear zone, pendant rocks are commonly east–west oriented with east–west foliations (Fig. 2). Pendant rock foliations are transposed to north–south *within* the PKCF zone. This is seen in foliations of the marble and schist limb stretching westward from the town of Fairview just south of the Durrwood Creek study area (Fig. 2, see plate 1 for location). The same marble and schist beds, within the PKCF zone, are stretched north–south over an 8–10 km length. This is also true for marble, quartzite, and schist just north of Lake Isabella.

On the northeastern shore of the lake, foliations of these metasedimentary rocks strike east–west. As these same rocks are caught in the PKCF damage zone to the west, their foliations become north–south oriented, and the rocks are stretched out over a distance >17 km (Plate 1). The aspect ratio of the schist limb stretching northward from the north shore of Lake Isabella is 1:17. In comparison with the more common 1:3 aspect ratios of pendant rock bodies outside of the PKCF zone, this pendant limb is stretched and transposed to a great degree along the shear zone.

Based on shear-strain studies of S-C mylonites, we place the lower limit of PKCF dextral displacement at 5 km. However, the lengths and aspect ratios of igneous intrusive bodies and metamorphic pendant rock bodies suggest a much greater displacement of up to 15 km occurred along the PKCF. In the next section, we attempt to analyze the stress levels that attended the ductile deformation of this shear zone.

Paleopiezometry

This section summarizes the concept of paleostress analyses, referred to as piezometry or paleopiezometry, based primarily on the works of Twiss (1977), Koch (1983), Ord and Christie (1984), Hacker et al. (1990 and 1992), Koch (1983), and conversations with Jim Dunlap at Australia National University and Greg Hirth at the Woods Hole Oceanographic Institute. The underlying principle on which piezometry is based is that dislocations form in crystals during plastic deformation. These dislocations create strain in the crystal lattice, imparting energy, and the greater the number of dislocations, the higher the strain energy of the crystal. Deformation mechanisms are described in the previous chapter, but to summarize here, the smaller the recrystallized

grains are, the higher the stress the rock was subjected to, since smaller grains can more effectively distribute internal energy over a larger surface area. Thus, the size of recrystallized grains can be used as a proxy for the deformation conditions under which the rock reorganized its grain boundaries. More recently, it was shown that dynamically recrystallized quartz grain size is independent of strain rate, water content, finite strain, temperature, and initial grain size (Koch, 1983).

Several natural factors can complicate the application of a grain size piezometer. The presence of other mineral phases (e.g., mica, feldspar, pyroxene) interfere with grain boundary migration, halting the growth of quartz grains and resulting in generally smaller grain sizes and an overestimation of paleostress (Haroun and Budworth, 1968; Christie and Ord, 1984). Annealing, a process by which high temperatures speed the removal of dislocations from a crystal lattice and allow growth of new, larger grains, results in an underestimation of paleostress (Twiss, 1977; Hacker et al., 1990, 1992). When a recrystallized, non-annealed, pure quartzite sample is found, the most important consideration is the dislocation creep regime in which the sample deformed. This depends on the relative rates of grain boundary migration, dislocation climb, and dislocation production (Hirth and Tullis, 1992). It is therefore imperative to determine what deformation mechanisms were responsible for the microstructures in question, so that flow laws appropriate to those mechanisms can be used to estimate the conditions of mylonite formation. Chapter 4 provided a detailed overview of such mechanisms for the northern segment of the PKCF. In this region of the fault, the presence of flattened grains and subgrain boundaries suggests simultaneous formation of quartz fabrics and of

dynamically recrystallized grains during mylonitization via the principal deformation mechanism of dislocation creep.

Procedure and Preparation

Although rock samples from the northern segment of the PKCF lack the pure quartz composition necessary to apply the quartzite piezometer confidently, the appropriate samples were found in the middle segment of the shear zone. The samples analyzed are from well-developed quartz mylonites of the PKCF near Cannell Creek and near Corral Creek (Fig. 3, see Plate 1 for locations). These samples were chosen for their purity of quartz content and for their grain textures that indicate dislocation creep as the primary deformation and recovery mechanism. For each sample, grain sizes were measured directly from thin sections by two different methods. In the first, 300 grains were measured both parallel and perpendicular to the trace of foliation along five transects of 60 grains each. The actual grain diameter (D) is 3/2 L, the measured mean grain size (Christie and Ord, 1980). In the second method, the average grain size was calculated from the relationship $3/2\ \sqrt[3]{(abc)}$, where a, b, and c are the number of grains per unit length on three different traverses across one thin section (DeHoff and Rheins, 1968). Flow stresses were then calculated using the piezometer of Koch (1983):

$$\sigma = Ad^{n} \tag{5}$$

where σ is the differential stress, d is the grain size in μm, and A and n are experimentally determined constants (A = 4090, n = -1.11). These calculations were compared with the piezometer introduced by Twiss (1977):

$$\sigma = Bd^{-0.68} \tag{6}$$

where d is grain size in mm and B is 5.5 for quartz. Although the Koch (1983) piezometer is the most recent one, that of Twiss (1977) is just as valid and results from both of these calculations are shown for comparison (Table 1). Indeed, all of the available piezometers give similar flow stresses for grain sizes in the 10–100 μm range.

Results

Grain Sizes

Individual quartz grains in sample 91SS27B from the Corral Creek area range in size from 38 μm to 113 μm. Both methods described above yield similar *average* grain diameters of 69 μm and 63 μm, respectively. Quartz grains in sample 89SS14 from the Cannell Creek area are longer than they are wide, with aspect ratios ranging between 1:1 and 9:1. These stretched grains thus yield a greater span in grain diameters, from 60 μm to 233 μm. The two methods of determining average quartz grain diameter correspondingly yield different results for this sample, of 89 μm and 140 μm, respectively. It is possible that some post-deformational annealing allowed grain growth in this sample, and the measured grain sizes could be larger than the grain sizes developed during mylonitization. Nonetheless, the Cannell Creek sample is nearly twice as coarse as the Corral Creek sample, implying that differential stress or thermal cooling histories were different for these two samples.

Differential Stress During Mylonitization

The piezometers of both Koch (1983) and Twiss (1977) are in good agreement with each other for both samples analyzed. The recrystallized grain size piezometer of

Koch (1983) is preferred because it is based on data from experiments on both "wet" and "dry" quartzite deformed over a wide range of pressures, temperatures, and strain rates. Differential stresses for quartzite from Corral Creek (91SS27B) are 37–41 MPa according to the Koch (1983) piezometer, and 34–36 MPa according to the Twiss (1977) piezometer. Differential stresses for the quartzite from Cannell Creek (89SS14) are somewhat lower, at 17–28 MPa for the Koch (1983) piezometer and 21–29 MPa for the Twiss (1977) piezometer. Because grain sizes in this sample may have increased during post-deformational annealing, these calculated differential stresses are lower limits to the stress during mylonitization. These two samples from the PKCF suggest that mylonitization occurred under differential stresses (σ_1 - σ_3) of 20–40 MPa, or shear stresses of 10–20 MPa. While paleostress studies of near-vertical, strike-slip shear zones are lacking, similar studies in ductile thrust sheets typically range between 10 and 250 MPa (Ord and Christie, 1984; Hacker et al., 1990, 1992; Dunlap, 1992).

Strain Rates During Mylonitization

Differential stress determined from dynamically recrystallized quartz grains can be combined with temperature estimates to determine the strain rate during ductile deformation. This result can be achieved by using published flow laws for quartzite deformed by dislocation creep. These flow laws follow the form:

$$\varepsilon = A\sigma^n \exp(-Q/RT) \quad (7)$$

and in this analysis, the experimentally determined parameters of Paterson and Luan (1990) will be applied (these are: $A = 6.5*10^{-8}$ MPa^{-n} s^{-1}; $n = 3.1$; $Q = 135$ kJ mol^{-1}). Using the differential stresses of 20–40 MPa calculated above, and assigning a 400˚–500˚

C temperature range to late-stage deformation along the PKCF near the contact with intruding magmas (see also Chapter 4), we calculate the strain rate along the middle section of the PKCF to have been between $4.5*10^{-12}$ s^{-1} to $2.3*10^{-14}$ s^{-1}. A lower temperature yields a slower strain rate, as does a lower differential stress. These results are similar to strain rates calculated from mylonites of other ductile faults (Ord and Christie, 1984; Hacker et al., 1990, 1992; Dunlap, 1992; Chapter 4).

Discussion and Conclusions

The structures and microstructures that document flow stress and strain along the PKCF are the products of an extended deformation history that involved early vertical ductile thrusting followed closely by dextral strike-slip ductile shearing, and finally by brittle dextral faulting. Early, east–west oriented fabrics lie just outside of the deformation zone of the PKCF, and these are transposed to north–south by the shear zone. Although shear-strain analyses of S-C mylonites suggest dextral slip of ~5 km, the north–south stretching of igneous bodies and metamorphic pendant rocks along the PKCF suggest dextral slip of up to 15 km. These rocks, which are elongated to aspect ratios of up to 1:17 (a difficult figure to assign with confidence), underwent significant straining within the middle segment of the PKCF, near the latitude of Lake Isabella. Outside of the main damage zone of the fault, igneous plutons and metamorphic pendants are typically more round, and in some cases are even east–west elongate.

Dynamically recrystallized quartz grains from pure quartzite mylonites along the PKCF were used to determine flow stresses during deformation. Piezometry studies yielded stresses of 20–40 MPa along the middle segment of the PKCF, and these were

applied, along with deformation temperature estimates of 400˚–500˚ C to estimate strain rates of 10^{-12} s^{-1} to 10^{-14} s^{-1} along the shear zone. It would be interesting to apply the piezometric and strain rate study to rocks along the length of the shear zone, especially in the southern reaches, to see if stress and strain rate vary as a function of depth along the PKCF.

References

Christie, J. M., Ord, A., and Koch, P. S., 1980, Relationship between recrystallized grain size and flow stress in experimentally deformed quartzite: *EOS Trans*., v. 61, p. 377.

DeHoff, R. T., and Rheins, F. N., 1968, Quantitative microscopy: New York, McGraw-Hill, 422 pp.

Dunlap, J., 1992, Structure, kinematics, and cooling history of the Arltunga nappe complex, central Australia: *PhD thesis,* University of Minnesota, 270 pp.

Hacker, B. R., Yin, A., and Christie, J. M., 1990, Differential stress, strain rate, and temperatures of mylonitization in the Ruby Mountains, Nevada: Implications for the rate and duration of uplift: *Jour. of Geophys. Res*., v. 95, n. B6, p. 8569-8580.

Hacker, B. R., Yin, A., Christie, J. M., and Davis, G. A., 1992, Stress magnitude, strain rate, and rheology of extended middle continental crust inferred from quartz grain sizes in the Whipple Mountains, California: *Tectonics*, v. 11, n. 1, p. 36-46.

Hirth, G., and Tullis, J., 1992, Dislocation creep regimes in quartz aggregates: Jour. of Struct. Geol., v. 14, p. 145-160.

Koch, P. S., 1983, Rheology and microstructures of experimentally deformed quartz aggregates: *PhD thesis*, University of California, Los Angeles.

Mercier, J. C., Anderson, D., and Carter, N. L., 1977, Stress in the lithosphere: Inferences from steady-state flow of rocks: *Pure and Applied Geophysics*, v. 115, p. 199-226.

Ord, A., and Christie, J. M., 1984, Flow stresses from microstructures in mylonitic quartzites of the Moine thrust zone, Assynt area, Scotland: *Jour. of Struct. Geol*., v. 6, n. 6, p. 639-654.

Ramsay, J. G., and Graham, R. H., 1970, Strain variation in shear belts: *Can. Jour. of*

Earth Sci., v. 7, p. 786-813.

Twiss, R. J., 1977, Theory and applicability of a recrystallized grain size paleopiezometer: *Pure and Applied Geophysics*, v. 115, p. 228-224.

Figure Captions

1. Shear strain–displacement study for a) Corral Creek, located just east of sample location 91SS27 on Plate 1, and b) Cannell Creek, located just east of sample location 89SS14 on Plate 1.

2. Foliations and small fold axes of the metamorphic pendant rocks near the town of Fairview (see Plate 1 for location). East-west striking foliations are transposed to north-south by the PKCF. Steeply dipping foliations and steeply dipping fold axis lineations suggest all structures were affected by vertical stretching.

3. Recrystallized quartz grains of a) Sample 89SS14, and b) Sample 91SS27 used for piezometry study. See Plate 1 for sample locations.

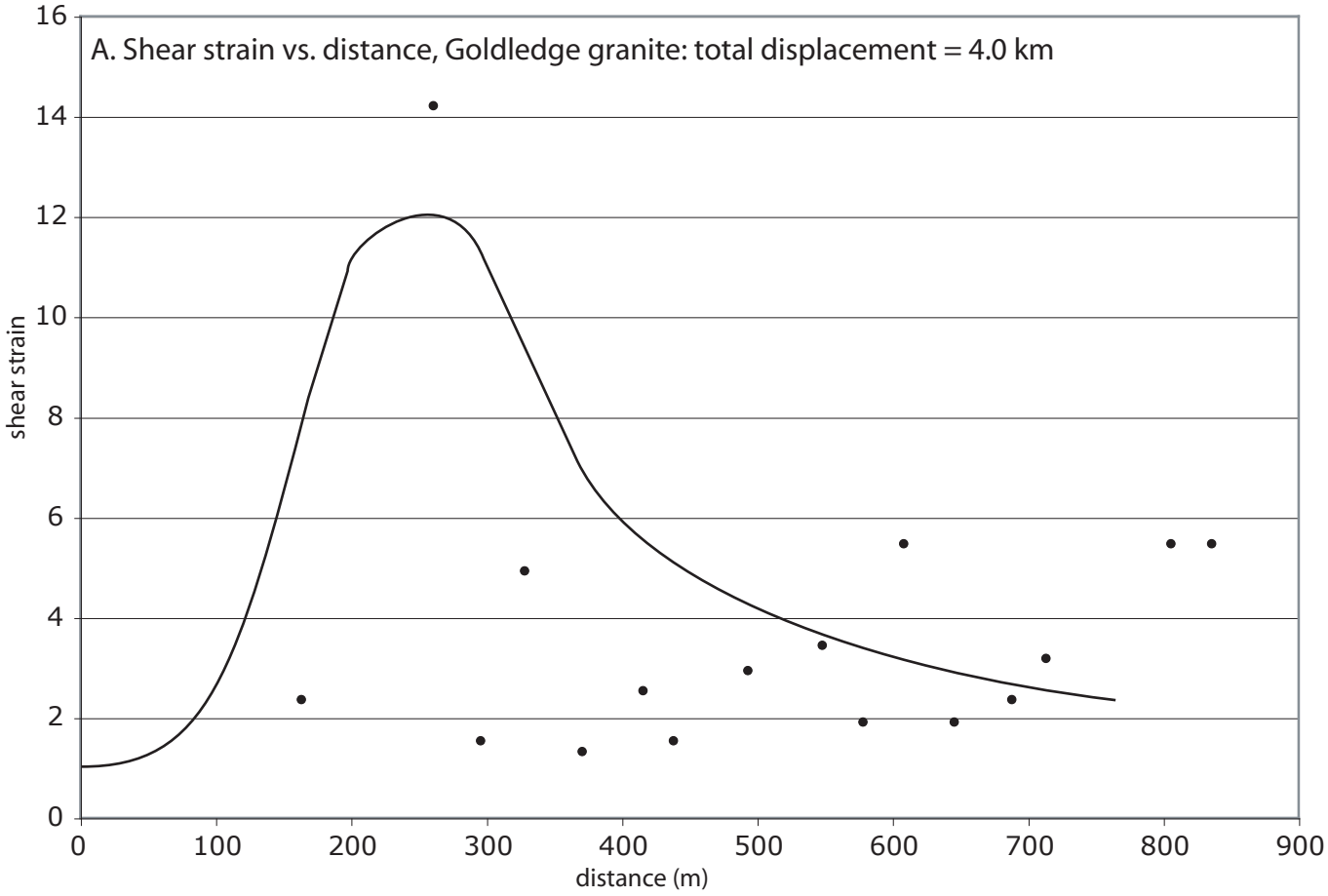
A. Shear strain vs. distance, Goldledge granite: total displacement = 4.0 km
shear strain
distance (m)
0
2
4
6
8
10
12
14
16
0
100
200
300
400
500
600
700
800
900

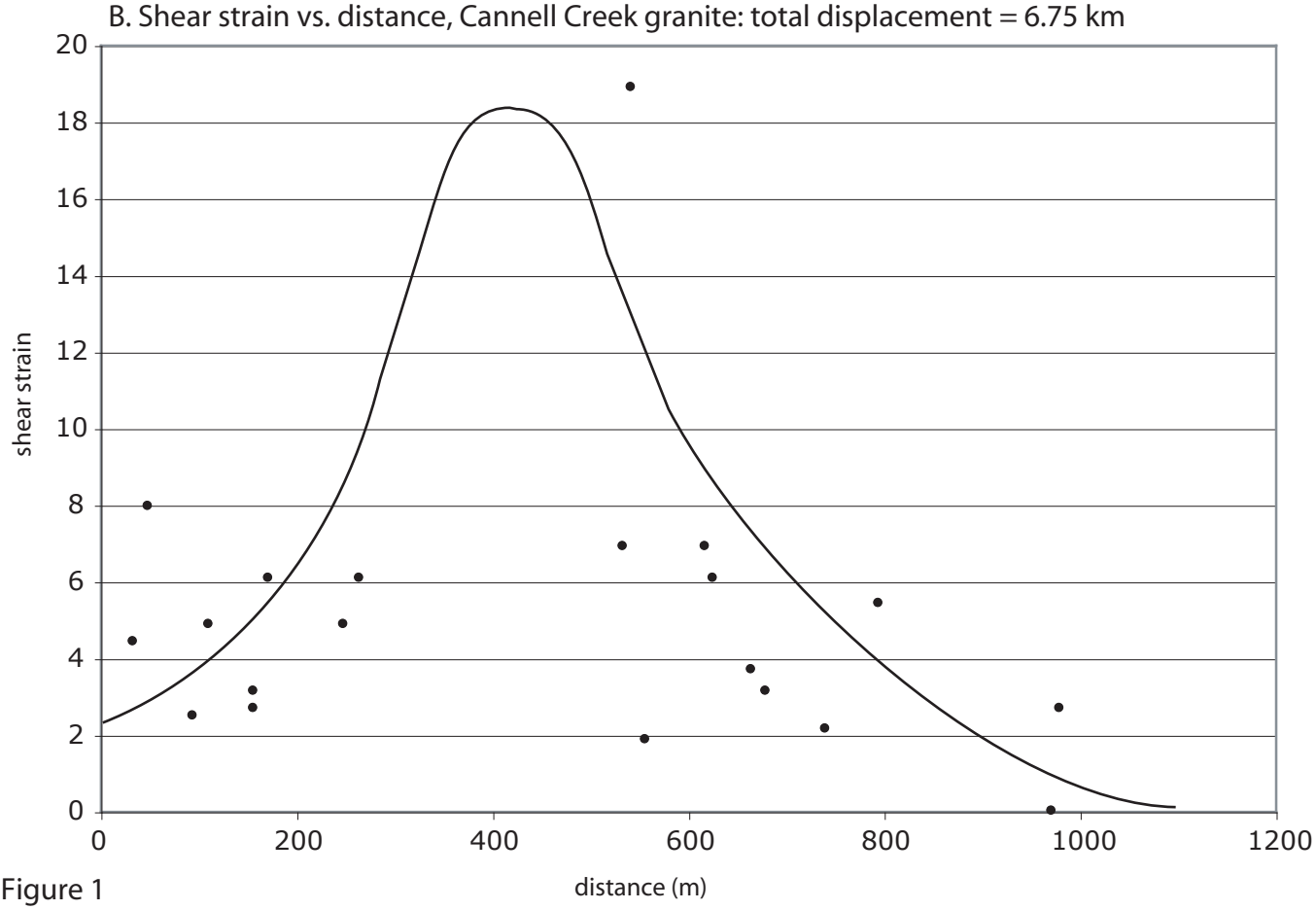
B. Shear strain vs. distance, Cannell Creek granite: total displacement = 6.75 km
shear strain
distance (m)
0
2
4
6
8
10
12
14
16
18
20
0
200
400
600
800
1000
1200

Figure 1

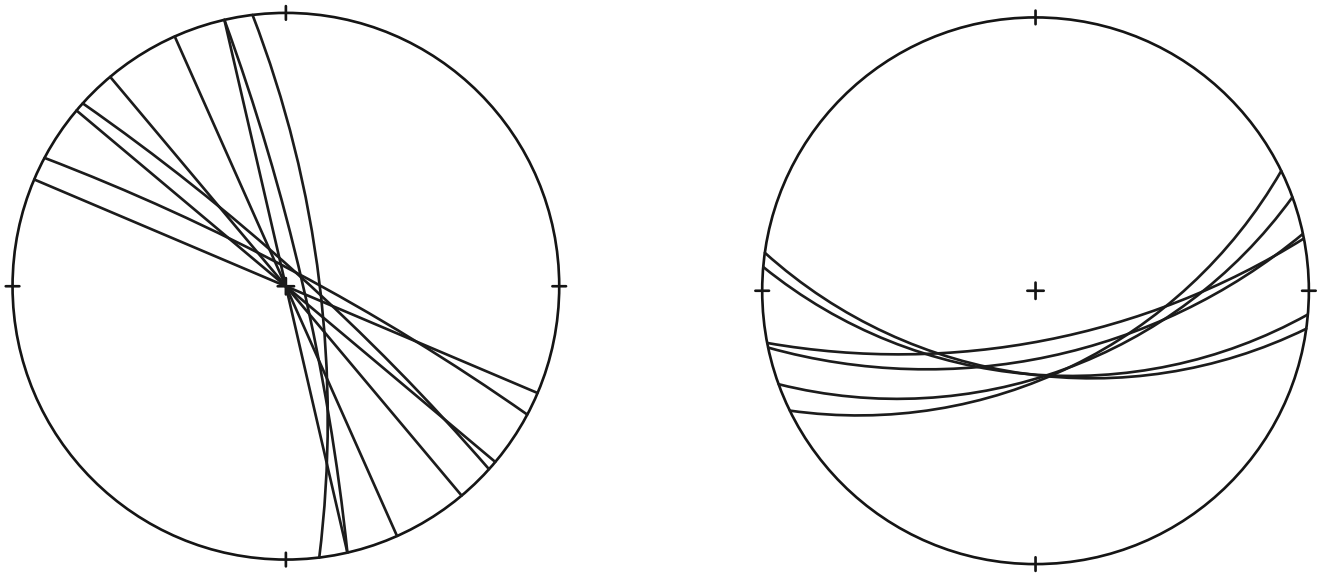

Foliations and small fold axes,
central marble, Fairview limb

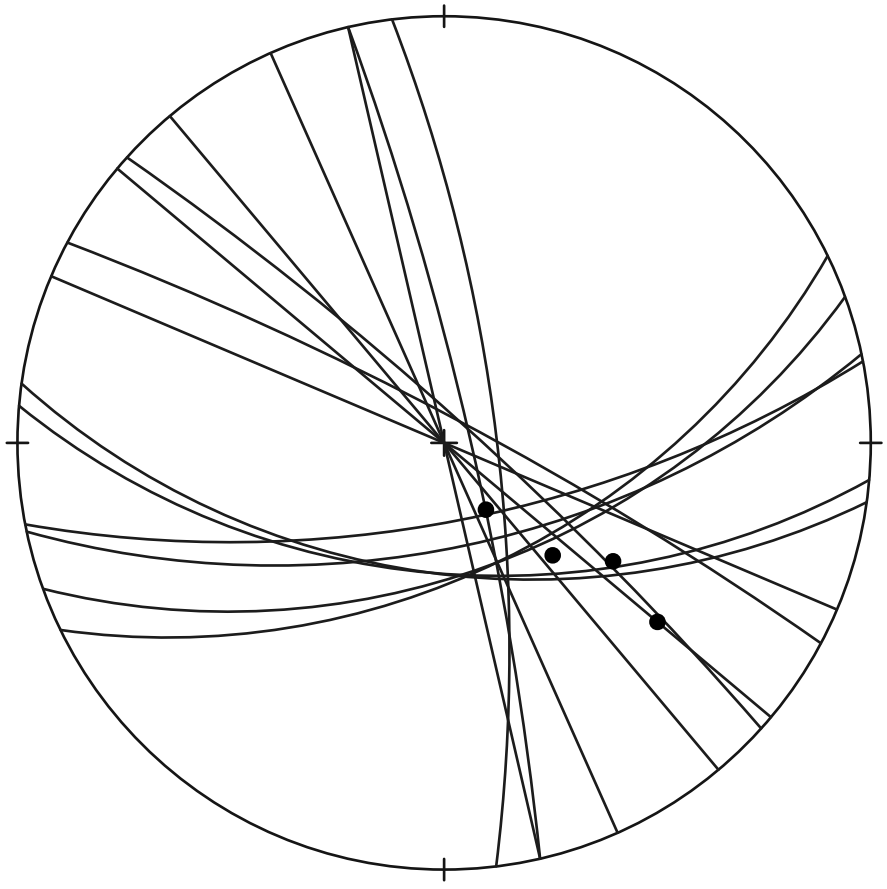

Figure 2

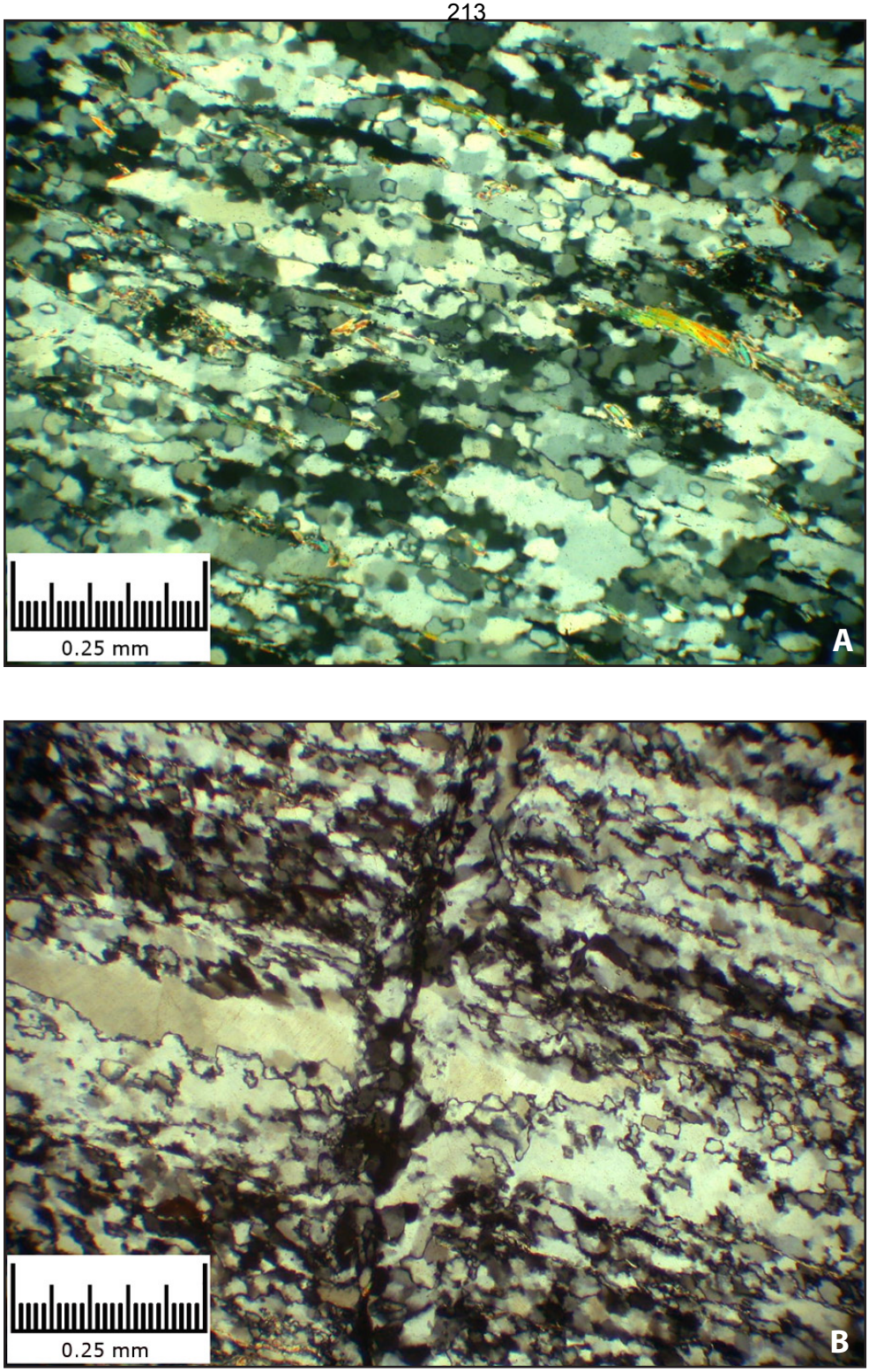

Figure 3. Recrystallized quartz grains of A) Sample 89SS14, and B) Sample 91SS27

Table 1.

91SS27B'		
average grain size (um)	**D (3/2 L)**	**3/2(abc)^1/3**
	69.3	62.8
Flow stress (Mpa)		
Twiss, 1977	33.8	36.1
Koch, 1983	37	41.3

89SS14		
average grain size (um)	**D (3/2 L)**	**3/2(abc)^1/3**
	139.9	88.6
Flow stress (Mpa)		
Twiss, 1977	21	28.6
Koch, 1983	17	28.2